

1 Cortical processing of breathing perceptions in the athletic brain

2 Olivia K. Faull^{1,2,3}, Pete J. Cox³, Kyle T. S. Pattinson^{1,2}

3

4 ¹FMRIB Centre and ²Nuffield Division of Anesthetics, Nuffield Department of Clinical
5 Neurosciences, University of Oxford, Oxford, UK, and ³Department of Physiology, Anatomy
6 and Genetics, University of Oxford, Oxford, UK

7

8

9 Running title: Athlete breathlessness brain networks

10 Key words: athletes, breathlessness, interoception, fMRI, ventilation

11

12

13 **Corresponding author:**

14 Dr Olivia Faull

15 Nuffield Department of Clinical Neurosciences

16 University of Oxford

17 Oxford, UK

18 Email: olivia.faull@ndcn.ox.ac.uk

19 Phone: +44 (0)1865 34544

20 Fax: +44 (0)1865 23079

21

22

23 **Abstract**

24 Athletes regularly endure large increases in ventilation, and accompanying perceptions of
25 breathlessness. While breathing perceptions often correlate poorly with objective measures of
26 lung function in both health and clinical populations, we have previously demonstrated closer
27 matching between subjective breathlessness and changes in ventilation in endurance athletes,
28 suggesting that athletes may be more accurate during respiratory interoception. To better
29 understand the link between exercise and breathlessness, we sought to identify the mechanisms
30 by which the brain processing of respiratory perception might be optimised in athletes.

31 Twenty endurance athletes and 20 sedentary controls underwent 7 Tesla functional
32 magnetic resonance imaging. Inspiratory resistive loading induced conscious breathing
33 perceptions (breathlessness), and a delay-conditioning paradigm was employed to evoke
34 preceding periods of anticipation. Athletes demonstrated anticipatory brain activity that
35 positively correlated with resulting breathing perceptions within key interoceptive areas, such as
36 the thalamus, insula and primary sensorimotor cortices, which was negatively correlated in
37 sedentary controls. Athletes also exhibited greater connectivity between interoceptive attention
38 networks and primary sensorimotor cortex. These functional differences in athletic brains
39 suggest that exercise may optimise processing of respiratory sensations. Future work may probe
40 whether these brain mechanisms are harnessed when exercise is employed to treat breathlessness
41 within chronic respiratory disease.

42 Introduction

43 Athletes are able to undertake incredible feats of human achievement, with faster, higher and
44 stronger performances recorded each year. Whilst exercise training is known to induce
45 widespread physiological changes in the periphery, the concurrent changes in the structure and
46 function of the athletic brain are less well investigated. For endurance athletes, exercise training
47 is targeted to improve the ability of tissues to utilize oxygen in the combustion of fuels such as
48 fat and carbohydrate, producing the energy required for repeated skeletal muscle contraction
49 (Holloszy & Coyle, 1984; Jones & Carter, 2000). However, the role of the brain in perceiving
50 and modulating changing sensations from the periphery, useful for maintenance of homeostasis
51 during situations of perturbed physiology, is often overlooked.

52 Ventilation during exercise is tightly controlled, balancing neurally-modulated feed
53 forward ventilatory commands and peripheral feedback to stimulate appropriate ventilation for
54 exercising needs (Kaufman & Forster, 1996; Waldrop *et al.*, 2010). Interoceptive monitoring of
55 respiratory sensations contributes to the maintenance of homeostasis (Davenport & Vovk, 2009),
56 and with sufficient exercise intensity, the strain of immense increases in ventilation induces
57 perceptions of breathlessness (El-Manshawi *et al.*, 1986; Takano *et al.*, 1997; Lansing *et al.*,
58 2000; Borg *et al.*, 2010). While endurance athletes are repeatedly exposed to these respiratory
59 sensations and breathlessness, it is as yet unknown whether brain networks involved in these
60 perceptions may also adapt to better cope with exercise demands. This understanding would
61 allow us to explore how processing of ventilatory signals might be altered in different states,
62 such as in athletes or conversely in chronic respiratory disease, where subjective reports of
63 breathlessness are often discordant with objective measures of lung function and ventilation
64 (Herigstad *et al.*, 2017).

65 Importantly, prior experiences of strong respiratory sensations may also alter the way
66 someone anticipates and perceives their breathing (Faull *et al.*, 2017; Van den Bergh *et al.*, 2017;
67 Herigstad *et al.*, 2017). Expectations regarding upcoming respiratory sensations from
68 conditioned cues (Pavlov, 1927), for example the breathlessness associated with an approaching
69 hill whilst running, can be an important influence on both threat behaviours and preventative
70 actions (i.e. to avoid the hill) (Lang *et al.*, 2011), or on the perception itself (Price *et al.*, 1999;
71 Porro *et al.*, 2002; Wager *et al.*, 2004). Repeated breathlessness exposure may alter this
72 anticipation in athletes, focusing their attention towards respiratory sensations (Merikle &
73 Joordens, 1997; Phelps *et al.*, 2006; Ling & Carrasco, 2006), reducing their anxiety (Spinhoven
74 *et al.*, 1997; Bogaerts *et al.*, 2005; Tang & Gibson, 2005) or improving their interoceptive ability
75 (Gray *et al.*, 2007; Critchley *et al.*, 2013; Mallorqui-Bague *et al.*, 2016; Garfinkel *et al.*, 2016b;
76 2016a). Interestingly, exercise therapy is currently the most effective treatment for
77 breathlessness associated with chronic obstructive pulmonary disease (COPD), improving
78 breathlessness intensity and anxiety (Carrieri-Kohlman *et al.*, 1996; 2001; Herigstad *et al.*,
79 2017), without concurrent improvements in lung function. It is possible that athletes may have
80 different prior expectations and anticipation of breathlessness, although this has yet to be
81 investigated.

82 In previous work we have observed closer matching between changes in ventilation and
83 perceptions of breathlessness in endurance athletes compared to sedentary individuals (Faull *et*
84 *al.*, 2016a). Here, we sought to identify how the brain processing of both anticipation and
85 perception of respiratory sensations may be altered in these athletes, to better understand
86 potential contributors to ventilatory interoception. We investigated functional brain activity using
87 magnetic resonance imaging (fMRI) during both conditioned anticipation and perception of a

88 breathlessness stimulus. We also examined potential differences in the resting temporal
89 coherence, or ‘functional connectivity’ (Gerstein & Perkel, 1969; Van Den Heuvel & Pol, 2010)
90 of brain networks involved in attention towards sensory information, allostasis and interoception
91 (Kleckner *et al.*, 2017). Differences in underlying functional connectivity may help us to
92 understand how the athlete brain may be altered to facilitate accurate respiratory perceptions, and
93 we hypothesized that these athletes would demonstrate both altered functional breathlessness-
94 related brain activity and connectivity compared to their sedentary counterparts.

95

96

97 **Materials and Methods**

98 **Subjects**

99 The Oxfordshire Clinical Research Ethics Committee approved the study and volunteers gave
100 written, informed consent. Forty healthy, right-handed individuals undertook this study, with no
101 history of smoking or any respiratory disease. This cohort comprised two groups; 20 subjects
102 who regularly participated in endurance sport, and 20 age- and sex-matched (± 2 years) sedentary
103 subjects (in each group: 10 males, 10 females; mean age \pm SEM, 26 ± 1.7 years). Athletes were
104 active participants in endurance sports (cycling, rowing and endurance running), with training
105 sessions conducted at least 5 times per week. Sedentary subjects did not partake in any regular
106 exercise or sport. Prior to scanning, all subjects underwent breathlessness testing during exercise
107 and chemostimulated hyperpnea, which have been presented elsewhere (Faull *et al.*, 2016a), and
108 a combined whole-group analysis of fMRI data has been previously reported (Faull & Pattinson,
109 2017).

110

111 **Stimuli and tasks**

112 Subjects were trained using an aversive delay-conditioning paradigm to associate simple shapes
113 with an upcoming breathlessness (inspiratory resistance) stimulus (Faull & Pattinson, 2017). A
114 breathing system was used to remotely administer periods of inspiratory resistive loading to
115 induce breathlessness (as predicted by the conditioned cues). The breathing system contained an
116 inspiratory resistance arm (using a porous glass disk) with a non-rebreathing valve connected to
117 a mouth piece, which could be periodically applied using the addition or removal of medical air
118 through an alternative inspiratory non-rebreathing arm (detailed in (Faull et al., 2016b; Faull &
119 Pattinson, 2017)). Mean peak inspiratory resistance was recorded at 14.7 (± 8.3) cmH₂O for the
120 loading periods across subjects, and group values are presented in Tables 1 and 2. The subject's
121 nose was blocked using foam earplugs and they were asked to breathe through their mouth for
122 the duration of the experiment.

123 Two conditions were trained: 1) A shape that always predicted upcoming breathlessness
124 (100% contingency pairing), and 2) A shape that always predicted unloaded breathing (0%
125 contingency pairing with inspiratory resistance). The 'certain upcoming breathlessness' symbol
126 was presented on the screen for 30 s, which included a varying 5-15 s anticipation period before
127 the loading was applied. The 'unloaded breathing' symbol was presented for 20 s, and each
128 condition was repeated 14 times in a randomised order. Conscious associations between cue and
129 threat level (cue contingencies) were required and verified in all subjects by reporting (in
130 writing) the meaning of each of the symbols both following the training session and immediately
131 prior to the MRI scan.

132 Rating scores of breathing intensity were recorded after every stimulus, using a visual-
133 analogue scale (VAS) with a sliding bar to answer the question 'How difficult was the previous

134 stimulus?’ where the subjects moved between ‘Not at all difficult’ (0%) and ‘Extremely difficult’
135 (100%). Subjects were also asked to rate how anxious each of the symbols made them feel
136 (‘How anxious does this symbol make you feel?’) using a VAS between ‘Not at all anxious’
137 (0%) and ‘Extremely anxious’ (100%) immediately following the functional MRI protocol.

138

139 **Physiological measurements**

140 We used established methods to decorrelate the effects of hypercapnia from the localised BOLD
141 responses associated with breathing against an inspiratory resistance, using additional, matched
142 carbon dioxide (CO₂) boluses interspersed during rest periods in the fMRI protocols as
143 previously described (Pattinson *et al.*, 2009b; Faull *et al.*, 2015; 2016b). In addition, a mildly
144 hyperoxic state was achieved through a constant administration of oxygen at a rate of 0.5 L/min,
145 to minimise fluctuations in end-tidal oxygen (P_{ET}O₂) (Table 1). Physiological measures were
146 recorded continuously using respiratory bellows surrounding the chest, and heart rate was
147 measured using a pulse oximeter (9500 Multigas Monitor, MR Equipment Corp., NY, USA)
148 during the training session and MRI scan, as previously described (Faull *et al.*, 2016b).

149

150 **MRI scanning sequences**

151 MRI was performed with a 7 T Siemens Magnetom scanner, with 70 mT/m gradient strength and
152 a 32 channel Rx, single channel birdcage Tx head coil (Nova Medical).

153 *BOLD scanning:* A T2*-weighted, gradient echo EPI was used for functional scanning.
154 The field of view (FOV) covered the whole brain and comprised 63 slices (sequence parameters:
155 TE, 24 ms; TR, 3 s; flip angle, 90°; voxel size, 2 x 2 x 2 mm; field of view, 220 mm; GRAPPA
156 factor, 3; echo spacing, 0.57 ms; slice acquisition order, descending), with 550 volumes (scan

157 duration, 27 mins 30 s) for the task fMRI, and 190 volumes (scan duration, 9 mins 30 s) for a
158 following resting-state acquisition (eyes open).

159 *Structural scanning:* A T1-weighted structural scan (MPRAGE, sequence parameters:
160 TE, 2.96 ms; TR, 2200 ms; flip angle, 7°; voxel size, 0.7 x 0.7 x 0.7 mm; field of view, 224 mm;
161 inversion time, 1050 ms; bandwidth, 240 Hz/Px) was acquired. This scan was used for
162 registration of functional images.

163 *Additional scanning:* Fieldmap scans (sequence parameters: TE1, 4.08 ms; TE2, 5.1 ms;
164 TR, 620 ms; flip angle, 39°; voxel size, 2 x 2 x 2 mm) of the B_0 field were also acquired to assist
165 distortion-correction.

166

167 **Physiological data analysis**

168 Values for end-tidal CO_2 ($P_{ET}CO_2$) were extrapolated for use as noise regressor in fMRI analysis
169 (explained below). Respiratory waveforms, respiratory volume per unit time (RVT) and cardiac
170 pulse oximetry triggers were included in the image denoising procedures (explained below),
171 Values for mean and peak resistive loading, mean $P_{ET}CO_2$ and $P_{ET}O_2$, respiratory rate and RVT
172 were calculated across each time block using custom written scripts in MATLAB (R2013a, The
173 Mathworks, Natick, MA). Measures were averaged across each subject in each condition
174 (unloaded breathing, anticipation and breathlessness). Peak mouth pressure was also calculated
175 in each block and averaged in each subject for the resistive loading condition. Mean peak mouth
176 pressure, breathlessness intensity and breathlessness anxiety ratings were then compared
177 between the two groups using a student's paired T-test.

178

179 **Imaging analysis**

180 *Preprocessing*: Image processing was performed using the Oxford Centre for Functional
181 Magnetic Resonance Imaging of the Brain Software Library (FMRIB, Oxford, UK; FSL version
182 5.0.8; <http://www.fmrib.ox.ac.uk/fsl/>). The following preprocessing methods were used prior to
183 statistical analysis: motion correction and motion parameter recording (MCFLIRT (Jenkinson *et*
184 *al.*, 2002)), removal of the non-brain structures (skull and surrounding tissue) (BET (Smith,
185 2002)), spatial smoothing using a full-width half-maximum Gaussian kernel of 2 mm, and high-
186 pass temporal filtering (Gaussian-weighted least-squares straight line fitting; 120 s). B_0 field
187 unwarping was conducted with a combination of FUGUE and BBR (Boundary-Based-
188 Registration; part of FEAT: FMRI Expert Analysis Tool, version 6.0 (Greve & Fischl, 2009)).
189 Data denoising was conducted using a combination of independent components analysis (ICA)
190 and retrospective image correction (RETROICOR) (Harvey *et al.*, 2008; Brooks *et al.*, 2013)
191 using the externally recorded physiological measures (as previously described (Faull *et al.*,
192 2016b)), and included simultaneous regression of motion parameters.

193 *Image registration*: Following preprocessing, the functional scans were registered to the
194 MNI152 (1x1x1 mm) standard space (average T1 brain image constructed from 152 normal
195 subjects at the Montreal Neurological Institute (MNI), Montreal, QC, Canada) using a two-step
196 process: 1) Registration of subjects' whole-brain EPI to T1 structural image was conducted using
197 BBR (6 DOF) with (nonlinear) fieldmap distortion-correction (Greve & Fischl, 2009), and 2)
198 Registration of the subjects' T1 structural scan to 1 mm standard space was performed using an
199 affine transformation followed by nonlinear registration (FNIRT) (Andersson *et al.*, 2007).

200 *Functional voxelwise and group analysis*: Functional data processing was performed
201 using FEAT (FMRI Expert Analysis Tool), part of FSL. The first-level analysis in FEAT
202 incorporated a general linear model (Woolrich *et al.*, 2004), with the following regressors:

203 Resistive loading periods (calculated from physiological pressure trace as onset to termination of
204 each application of resistance); anticipation of breathlessness (calculated from onset of
205 anticipation symbol to onset of resistance application); and unloaded breathing (onset and
206 duration of ‘unloaded breathing’ symbol). Additional regressors to account for relief from
207 breathlessness, periods of rating using the button box, demeaned ratings of intensity between
208 trials, and a period of no loading following the final anticipation period (for decorrelation
209 between anticipation and breathlessness) were also included in the analysis. A final $P_{ET}CO_2$
210 regressor was formed by linearly extrapolating between end-tidal CO_2 peaks, and included in the
211 general linear model to decorrelate any $P_{ET}CO_2$ -induced changes in BOLD signal from the
212 respiratory tasks (McKay *et al.*, 2008; Pattinson *et al.*, 2009a; 2009b; Faull *et al.*, 2015; 2016b).
213 Contrasts for breathlessness (vs. baseline) and differential contrasts of anticipation of
214 breathlessness > unloaded breathing (referred to as ‘anticipation’ or ‘anticipation of
215 breathlessness’) were investigated at the group level.

216 Functional voxelwise analysis incorporated HRF modeling using three FLOBS regressors
217 to account for any HRF differences caused by slice-timing delays, differences across the
218 brainstem and cortex, or between individuals (Handwerker *et al.*, 2004; Devonshire *et al.*, 2012).
219 Time-series statistical analysis was performed using FILM, with local autocorrelation correction
220 (Woolrich *et al.*, 2001). The second and third waveforms were orthogonalised to the first to
221 model the ‘canonical’ HRF, of which the parameter estimate was then passed up to the group
222 analysis in a mixed-effects analysis. Group analysis was conducted using rigorous permutation
223 testing of a General Linear Model (GLM) using FSL’s Randomize tool (Winkler *et al.*, 2014),
224 where the GLM consisted of group mean BOLD activity for each group, and demeaned,
225 separated breathlessness intensity and anxiety covariates for each group. Including

226 breathlessness scores into the anticipation contrast allows us to identify preparatory brain activity
227 that predicts the subsequent breathlessness perception when the stimulus is applied. Mean
228 voxelwise differences between groups were calculated, as well as the interactions between group
229 and breathlessness intensity / anxiety scores. A stringent initial cluster-forming threshold of $t =$
230 3.1 was used, in light of recent reports of lenient thresholding previously used in fMRI (Eklund
231 *et al.*, 2016), and images were family-wise-error (FWE) corrected for multiple comparisons.
232 Significance was taken at $p < 0.05$ (corrected).

233 *Resting functional connectivity analysis:* Following preprocessing and image registration,
234 resting state scans from all subjects were temporally concatenated and analysed using
235 independent component analysis (ICA) using MELODIC (Beckmann & Smith, 2004), part of
236 FSL. ICA decomposes the data into a set of spatial maps and their associated timecourses,
237 referred to as ‘functional networks’. Model order in the group ICA was set to 25 spatially
238 independent components. Dual regression (Beckmann *et al.*, 2009) was then used to delineate
239 subject-specific timecourses of these components, and their corresponding subject-specific
240 spatial maps. Subject-specific spatial maps were again analysed non-parametrically using
241 Randomise (part of FSL) (Winkler *et al.*, 2014) with the same GLM and significance thresholds
242 previously applied to the functional task group analysis. Twenty components were identified as
243 signal, and two components of interest (‘default mode’ network and ‘task positive’ network)
244 were considered for group differences, in accordance with recent interoceptive research
245 (Kleckner *et al.*, 2017). Therefore, p threshold significance was adjusted to $p < 0.025$ using
246 Bonferroni correction for multiple comparisons.

247

248

249 **Results**

250 **Physiology and psychology of breathlessness**

251 Mean physiological values for each group for mouth pressure, $P_{ET}CO_2$, $P_{ET}O_2$, RVT, respiratory
252 rate and RVT are presented in Table 1. Group scores for breathlessness intensity and anxiety are
253 presented in Table 2, with no mean differences observed between groups. Previously, we have
254 reported a difference in the accuracy between subjective breathlessness scores and changes in
255 ventilation induced via a hypercapnic challenge (Faull *et al.*, 2016a) in the same subjects used as
256 the current study. For clarity, we have reproduced the results here in Figure 4.

257

258 **Task fMRI analysis**

259 *Mean group differences:* Mean activity during anticipation of breathlessness in each group is
260 presented in Figure 1. In sedentary subjects, significantly increased BOLD activity was observed
261 in the right anterior insula, operculum and bilateral primary motor cortex, and decreased BOLD
262 activity in bilateral posterior cingulate cortex, precuneus, lateral occipital cortex, hippocampus,
263 parahippocampal gyrus and amygdala. In athletes, increased BOLD activity was observed in
264 bilateral anterior insula, operculum and primary motor cortex, and right supplementary motor
265 cortex, and decreased BOLD activity in bilateral precuneus, hippocampus, parahippocampal
266 gyrus and amygdala. No statistically significant voxelwise differences were observed between
267 group mean activities during anticipation of breathlessness (differentially contrasted against
268 unloaded breathing).

269 Mean activity during breathlessness in each group is presented in Figure 1. In sedentary
270 subjects, significantly increased BOLD activity was observed in the bilateral anterior and middle
271 insula, operculum, primary sensory and motor cortices, supplementary motor cortex,

272 supramarginal gyrus and cerebellar VI, and decreased BOLD activity in bilateral precuneus. In
273 athletes, significantly increased BOLD activity was observed in the right dorsolateral prefrontal
274 cortex, bilateral anterior and middle insula, operculum, primary sensory and motor cortices,
275 supplementary motor cortex, left visual cortex and cerebellar Crus-I, and decreased BOLD
276 activity in right amygdala, hippocampus and superior temporal gyrus. No statistically significant
277 voxelwise differences were observed between group mean activities during breathlessness.

278 *Subjective breathlessness scores:* The brain activity that correlated with breathlessness
279 scores of intensity and anxiety was compared between groups, to identify any interaction effects
280 (group x subjective score). Interaction effects establish that the difference between groups varies
281 as a function of the covariate (subjective scores). Athletes demonstrated widespread brain
282 activity positively correlating with (predicted) intensity scores during anticipation of
283 breathlessness (Figure 2), whilst those same areas had a negative correlation in sedentary
284 subjects (interaction). This included activity in the bilateral ventral posterolateral nucleus of the
285 thalamus, middle insula, and primary motor and sensory cortices, as well as left anterior insula.
286 In contrast, a small amount of activity in the right putamen and caudate nucleus correlated with
287 anxiety in sedentary subjects, but not in athletes during anticipation. No significant interactions
288 between groups were present for either intensity or anxiety during breathlessness perception.

289

290 **Resting state network connectivity**

291 Of the 25 resting state ‘networks’ identified in the group ICA analysis, 20 components were
292 identified to represent relevant signal (19 cortical, 1 cerebellar) while the remaining 5 were
293 labeled as noise (see supplementary material for a summary the 20 resting networks). Two
294 networks of interest were identified for group comparison analyses (as determined by Kleckner

295 et al., 2017): 1) The network most representative of the typical ‘default mode’, and 2) A network
296 containing components of previously identified visual and dorsal attention networks (Vossel *et*
297 *al.*, 2014), which was notably most similar to the breathing task contrasts (‘task-positive’
298 network) (Figure 3). When network connectivity was compared between athletes and controls,
299 athletes were found to have significantly greater ($p = 0.019$) connectivity of the task-positive
300 network to an area of primary motor cortex active during resistive loading (Figure 3).

301

302

303 **Discussion**

304 **Main findings**

305 We have identified a cohesive anticipatory brain network that predicts upcoming subjective
306 ratings of breathlessness in athletes. Comparatively, this brain activity was reversed (i.e.
307 negatively correlated with upcoming breathlessness ratings) in sedentary controls. Furthermore,
308 at rest, athletes demonstrated greater connectivity between an area of breathing-related primary
309 sensorimotor cortex, and a cingulo-opercular attention network that is strikingly similar to that
310 recently identified to be involved in allostatic-interoceptive processing (Kleckner *et al.*, 2017).

311 This network may therefore be integral within attention and processing of sensory signals related
312 to breathing. Increased connectivity between sensorimotor cortex and this brain network may
313 underlie the observed differences in anticipatory processing of respiratory signals, and the
314 improved ventilatory perceptive accuracy found in these endurance athletes.

315

316 **Breathlessness processing in athletes**

317 Endurance athletes have repeated episodes of elevated ventilation and perceptions of
318 breathlessness as part of their training. In previously published results (Faull *et al.*, 2016a), we
319 have demonstrated improved psychophysical matching between changes in chemostimulated
320 hyperventilation and subjective breathlessness perceptions in these athletes compared to matched
321 sedentary subjects (Figure 4). Therefore, whether by nature or nurture, these individuals appear
322 to have improved ventilatory perception accuracy. The reduced correlation between changes in
323 ventilation and perceptions of breathlessness demonstrated in sedentary subjects implies a
324 worsened ability to process respiratory sensations, which may be a risk factor for symptom
325 discordance in disease (Van den Bergh *et al.*, 2017).

326 In accordance with behavioural findings, here we have observed differences in the brain
327 processing of breathing perceptions in athletes. Specifically, a coherent network of brain activity
328 corresponding to breathlessness intensity scores was observed during anticipation in athletes,
329 which was reversed (negatively correlated) with subjective scores in sedentary subjects. This
330 network incorporates key areas involved in sensorimotor control and interoception, such as the
331 thalamus, insula and primary sensorimotor cortices (Feldman & Friston, 2010; Simmons *et al.*,
332 2012; Feldman Barrett & Simmons, 2015; Van den Bergh *et al.*, 2017). The opposing
333 relationship between brain activity and subjective scores in athletes and sedentary subjects
334 indicates a fundamental difference in preparatory, anticipatory brain activity directed towards
335 subjective perceptions between these groups, which occurs without any difference in overall
336 group mean brain activity. Conversely, sedentary subjects demonstrated activity corresponding
337 to anxiety scores in the ventral striatum (caudate nucleus and putamen) during anticipation of
338 breathlessness. The striatum has been previously linked with cardiovascular responses resulting

339 from social threat (Wager *et al.*, 2009), and may represent heightened threat responses in
340 sedentary subjects.

341 Interestingly, the intensity-related differences in brain activity were observed during the
342 anticipation period that preceded the actual perception of breathlessness. It is possible that
343 repeated increases in ventilation and breathlessness during training helps athletes improve the
344 accuracy of their breathing expectations for an upcoming stimulus, such as expecting to run up a
345 hill. Recent theories of symptom perception have proposed a comprehensive, Bayesian model
346 (Feldman Barrett & Simmons, 2015; Van den Bergh *et al.*, 2017), which includes a set of
347 perceptual expectations or ‘priors’. These expectations are combined with sensory information
348 from the periphery, for the brain to probabilistically produce the most likely resulting perception.
349 Furthermore, factors such as attention (Merikle & Joordens, 1997; Phelps *et al.*, 2006; Ling &
350 Carrasco, 2006) and interoceptive ability (Gray *et al.*, 2007; Critchley *et al.*, 2013; Mallorqui-
351 Bague *et al.*, 2016; Garfinkel *et al.*, 2016b) are thought to influence this system, either by
352 altering the prior expectations or incoming sensory information.

353 While previous research had identified reduced anterior insula activity during loaded
354 breathing in endurance athletes (Paulus *et al.*, 2012), we have not reproduced these findings
355 when employing more stringent fMRI statistics. Nevertheless, the proposal by Paulus and
356 colleagues (Paulus *et al.*, 2012) that athletes demonstrate more efficient minimization of the
357 body prediction error remains a very plausible possibility. Here, instead, we have observed
358 functional perception-related differences during anticipation of loaded breathing in endurance
359 athletes. Therefore, repeated exercise training in athletes may develop breathlessness
360 expectations (or priors) and better direct attention towards breathing sensations, improving the
361 robustness of the perceptual system to accurately infer the intensity of breathlessness.

362

363 **Differences in functional connectivity within the athletic brain**

364 Understanding differences in underlying communication between functional brain regions may
365 inform us as to why differences in functional activity, such as observed in these athletes during
366 anticipation of breathlessness, may arise. The temporal synchronicity of seemingly spontaneous
367 fluctuations in brain activity across spatially distinct regions can inform us of how ‘functionally
368 connected’ these disparate regions may be, and is thought to be related to the temporal coherence
369 of neuronal activity in anatomically distinct areas (Gerstein & Perkel, 1969; Van Den Heuvel &
370 Pol, 2010).

371 It is now well established that the brain can be functionally parsed into resting state
372 ‘networks’, where distinct brain regions are consistently shown to exhibit temporally similar
373 patterns of brain activity (Smith *et al.*, 2009; Miller *et al.*, 2016). While properties of these
374 resting state networks have been linked to lifestyle, demographic and psychometric factors
375 (Smith *et al.*, 2015; Miller *et al.*, 2016), here we have found connectivity differences between
376 athletes and sedentary subjects for a cingulo-opercular network. This network displays a very
377 similar spatial distribution to the pattern of activity observed during the breathlessness tasks
378 (‘task-positive’) (Figure 3), as well as the allostatic-interoceptive network recently identified by
379 Kleckner and colleagues (Kleckner *et al.*, 2017), and to previously reported networks of ventral
380 and dorsal attention (Fox *et al.*, 2005; 2006). Here, we have demonstrated greater functional
381 connectivity in athletes between an area of primary sensory and motor cortices that has
382 consistently been identified as active during tasks such as breath holds (Pattinson *et al.*, 2009b;
383 Faull *et al.*, 2015) and inspiratory resistances (Faull *et al.*, 2016b; Faull & Pattinson, 2017;
384 Hayen *et al.*, 2017). Therefore, it is possible that this greater connectivity in athletes between an

385 interoceptive attention network and primary sensorimotor cortex contributes to the processing of
386 incoming and outgoing respiratory information, and thus may also be related to more accurate
387 ventilatory perceptions.

388 Whilst this cross-sectional study is unable to determine whether endurance exercise
389 training *induces* these differences in brain function and connectivity, or whether these
390 individuals are biased towards training for endurance sports, this work provides intriguing
391 preliminary insight that the brain may undergo adaptation in conjunction with the periphery, to
392 more accurately process perceptions of bodily sensations such as breathlessness.

393

394 **Neuroimaging statistical considerations**

395 Extensive efforts were made within the analysis of this dataset to ensure only the most robust and
396 reliable results were reported. Firstly, physiological noise and potential motion artifacts need to
397 be specifically addressed when using breathing-related tasks, and these can be further
398 compounded at higher field strengths (Brooks et al., 2013). Here we employed rigorous noise
399 correction procedures, combining retrospective image correction of physiological parameters
400 (heart rate, ventilation and end-tidal carbon dioxide) with both extended motion parameter
401 regression and independent component analysis de-noising (Faull et al., 2016b; Hayen et al.,
402 2017). Secondly, recent work has revealed the potential leniency of previous fMRI statistical
403 methodologies and thresholds (Eklund et al., 2016). In this manuscript, we have utilized minimal
404 (2mm) spatial smoothing to maintain accurate localization of brain activity, and employed non-
405 parametric, permutation testing with a robust cluster threshold of 3.1 (Eklund et al., 2016), to
406 represent only the most reliable statistical results. Whilst these approaches forsake much of our
407 previously-reported activity within these breathing-related tasks (Faull & Pattinson, 2017), we

408 can have greater confidence in our reported differences between brain and behavior in athletes
409 and sedentary subjects.

410

411 **Potential clinical implications of altering breathlessness processing**

412 As discussed, prior expectations of breathlessness are now considered to be a major contributor
413 to symptom perception (Hayen *et al.*, 2013; Faull *et al.*, 2017; Van den Bergh *et al.*, 2017;
414 Geuter *et al.*, 2017; Herigstad *et al.*, 2017). Altering the accuracy of breathlessness perception
415 using exercise training may be of interest when treating individuals with habitual symptomology,
416 such as those with chronic obstructive pulmonary disease (COPD) or asthma. Recent research
417 has shown exercise training to reduce breathlessness intensity and anxiety in patients with
418 COPD, with corresponding changes in the brain's processing of breathlessness-related words
419 (Herigstad *et al.*, 2016; 2017). It has been proposed that exercise exposure alters breathlessness
420 expectations and priors in these patients, modifying symptom perception when it has become
421 discordant with physiology in chronic disease (Parshall *et al.*, 2012; Herigstad *et al.*, 2017). It is
422 also possible that exercise helps improve the processing of respiratory signals for more accurate
423 ventilatory interoception in these patients, allowing breathlessness perception to better match
424 respiratory distress. Future work investigating the link between exercise, ventilation and
425 breathlessness perception may yield another treatment avenue (via targeted exercises) to improve
426 patient quality of life in the face of chronic breathlessness.

427

428

429 **Conclusions**

430 In this study, we have demonstrated altered anticipatory brain processing of breathlessness
431 intensity in athletes compared to sedentary subjects. This altered functional brain activity may be
432 underpinned by increased functional connectivity between an interoceptive network related to
433 breathlessness, and sensorimotor cortex that is active during ventilatory tasks. These differences
434 in brain activity and connectivity may also relate to improvements in ventilatory perception
435 previously reported between these subject groups (Faull *et al.*, 2016a), and open the door to
436 investigating exercise as a tool to manipulate brain processing of debilitating breathing
437 symptoms, such as breathlessness in clinical populations.

438

439

440 **Acknowledgements**

441 This research was supported by the JABBS Foundation. This research was further supported by
442 the National Institute for Health Research, Oxford Biomedical Research Centre based at Oxford
443 University Hospitals NHS Trust and University of Oxford. Olivia K Faull was supported by the
444 Commonwealth Scholarship Commission.

445

446

447 **Competing interests**

448 KP has acted as a consultant for Nektar Therapeutics. The work for Nektar has no bearing on the
449 contents of this manuscript. KP is named as a co-inventor on a provisional UK patent application
450 titled “Use of cerebral nitric oxide donors in the assessment of the extent of brain dysfunction
451 following injury.”

452

453

454 **References**

455 Andersson JL, Jenkinson M & Smith S (2007). Non-linear registration, aka Spatial normalisation
456 FMRIB technical report TR07JA2. FMRIB Analysis Group of the University of Oxford.

457 Beckmann CF & Smith SM (2004). Probabilistic Independent Component Analysis for
458 Functional Magnetic Resonance Imaging. *IEEE Transactions on Medical Imaging* 23, 137–
459 152.

460 Beckmann CF, Mackay CE, Filippini N & Smith SM (2009). Group comparison of resting-state
461 FMRI data using multi-subject ICA and dual regression. *NeuroImage* 47, S148.

462 Bogaerts K, Notebaert K, Van Diest I, Devriese S, De Peuter S & Van den Bergh O (2005).
463 Accuracy of respiratory symptom perception in different affective contexts. *J Psychosom
464 Res* 58, 537–543.

465 Borg E, Borg G, Larsson K, Letzter M & Sundblad BM (2010). An index for breathlessness and
466 leg fatigue. *Scand J Med Sci Sports* 20, 644–650.

467 Brooks JCW, Faull OK, Pattinson KTS & Jenkinson M (2013). Physiological noise in brainstem
468 FMRI. *Front Hum Neurosci* 7, 623–13.

469 Carrieri-Kohlman V, Gormley JM, Douglas MK, Paul SM & Stulbarg MS (1996). Exercise
470 training decreases dyspnea and the distress and anxiety associated with it: monitoring alone
471 may be as effective as coaching. *Chest Journal* 110, 1526–1535.

472 Carrieri-Kohlman V, Gormley JM, Eiser S, Demir-Deviren S, Nguyen H, Paul SM & Stulbarg
473 MS (2001). Dyspnea and the affective response during exercise training in obstructive
474 pulmonary disease. *Nursing Research* 50, 136–146.

475 Critchley HD, Eccles J & Garfinkel SN (2013). Interaction between cognition, emotion, and the
476 autonomic nervous system. In *Autonomic Nervous System, Handbook of Clinical Neurology*,
477 pp. 59–77. Elsevier.

478 Davenport PW & Vovk A (2009). Cortical and subcortical central neural pathways in respiratory
479 sensations. *Respiratory physiology & neurobiology* 167, 72–86.

480 Devonshire IM, Papadakis NG, Port M, Berwick J, Kennerley AJ, Mayhew JEW & Overton PG
481 (2012). Neurovascular coupling is brain region-dependent. *NeuroImage* 59, 1997–2006.

482 Eklund A, Nichols TE & Knutsson H (2016). Cluster failure: Why fMRI inferences for spatial
483 extent have inflated false-positive rate. *PNAS* 113, 7900–7905.

484 El-Manshawi A, Killian KJ, Summers E & Jones NL (1986). Breathlessness during exercise with
485 and without resistive loading. *Journal of Applied Physiology* 61, 896–905.

486 Faull O, Hayen A & Pattinson K (2017). Breathlessness and the body: Neuroimaging clues for
487 the inferential leap. *Cortex*; DOI: 10.1101/117408.

488 Faull OK & Pattinson KT (2017). The cortical connectivity of the periaqueductal gray and the
489 conditioned response to the threat of breathlessness. *Elife* 6, 95.

490 Faull OK, Cox PJ & Pattinson KTS (2016a). Psychophysical Differences in Ventilatory
491 Awareness and Breathlessness between Athletes and Sedentary Individuals. *Front Physiol* 7,
492 195–199.

493 Faull OK, Jenkinson M, Clare S & Pattinson KTS (2015). Functional subdivision of the human
494 periaqueductal grey in respiratory control using 7 tesla fMRI. *NeuroImage* 113, 356–364.

495 Faull OK, Jenkinson M, Ezra M & Pattinson KTS (2016b). Conditioned respiratory threat in the
496 subdivisions of the human periaqueductal gray. *Elife*; DOI: 10.7554/elife.12047.

497 Feldman Barrett LF & Simmons WK (2015). Interoceptive predictions in the brain. *Nat Rev
498 Neurosci* 16, 419–429.

499 Feldman H & Friston KJ (2010). Attention, Uncertainty, and Free-Energy. *Front Hum Neurosci*
500 4, 1–23.

501 Fox MD, Corbetta M, Snyder AZ, Vincent JL & Raichle ME (2006). Spontaneous neuronal
502 activity distinguishes human dorsal and ventral attention systems (vol 103, pg 10046, 2006).
503 *Proceedings of the National Academy of Sciences* 103, 13560–13560.

504 Fox MD, Snyder AZ, Vincent JL, Corbetta M, Van Essen DC & Raichle ME (2005). The human
505 brain is intrinsically organized into dynamic, anticorrelated functional networks. *Proceedings
506 of the National Academy of Sciences* 102, 9673–9678.

507 Garfinkel SN, Manassei MF, Hamilton-Fletcher G, In den Bosch Y, Critchley HD & Engels M
508 (2016a). Interoceptive dimensions across cardiac and respiratory axes. *Philos Trans R Soc
509 Lond, B, Biol Sci* 371, 20160014–10.

510 Garfinkel SN, Tiley C, O'Keeffe S, Harrison NA, Seth AK & Critchley HD (2016b).
511 Discrepancies between dimensions of interoception in autism: Implications for emotion and
512 anxiety. *Biological Psychology* 114, 117–126.

513 Gerstein GL & Perkel DH (1969). Simultaneously recorded trains of action potentials: analysis
514 and functional interpretation. *Science* 164, 828–830.

515 Geuter S, Boll S, Eippert F & Büchel C (2017). Functional dissociation of stimulus intensity
516 encoding and predictive coding of pain in the insula. *Elife* 6, e24770.

517 Gray MA, Harrison NA, Wiens S & Critchley HD (2007). Modulation of Emotional Appraisal
518 by False Physiological Feedback during fMRI. *PLoS ONE* 2, e546.

519 Greve DN & Fischl B (2009). Accurate and robust brain image alignment using boundary-based

520 registration. *NeuroImage* 48, 63–72.

521 Handwerker DA, Ollinger JM & D'Esposito M (2004). Variation of BOLD hemodynamic
522 responses across subjects and brain regions and their effects on statistical analyses.
523 *NeuroImage* 21, 1639–1651.

524 Harvey AK, Pattinson KTS, Brooks JCW, Mayhew SD, Jenkinson M & Wise RG (2008).
525 Brainstem functional magnetic resonance imaging: Disentangling signal from physiological
526 noise. *Journal of Magnetic Resonance Imaging* 28, 1337–1344.

527 Hayen A, Herigstad M & Pattinson KTS (2013). Understanding dyspnea as a complex individual
528 experience. *Maturitas* 76, 45–50.

529 Hayen A, Wanigasekera V, Faull OK, Campbell SF, Garry PS, Raby SJM, Robertson J, Webster
530 R, Wise RG, Herigstad M & Pattinson KTS (2017). Opioid suppression of conditioned
531 anticipatory brain responses to breathlessness. *NeuroImage* 150, 383–394.

532 Herigstad M, Faull O, Hayen A, Evans E, Hardinge M, Wiech K & Pattinson KTS (2017).
533 Treating breathlessness via the brain: Mechanisms underpinning improvements in
534 breathlessness with pulmonary rehabilitation. *European Respiratory Journal*; DOI:
535 10.1101/117390.

536 Herigstad M, Hayen A, Reinecke A & Pattinson KTS (2016). Development of a dyspnoea word
537 cue set for studies of emotional processing in COPD. *Respiratory physiology &*
538 *neurobiology* 223, 37–42.

539 Holloszy JO & Coyle EF (1984). Adaptations of Skeletal-Muscle to Endurance Exercise and
540 Their Metabolic Consequences. *Journal of Applied Physiology* 56, 831–838.

541 Jenkinson M, Bannister P, Brady M & Smith S (2002). Improved Optimization for the Robust
542 and Accurate Linear Registration and Motion Correction of Brain Images. *NeuroImage* 17,
543 825–841.

544 Jones AM & Carter H (2000). The Effect of Endurance Training on Parameters of Aerobic
545 Fitness. *Sports Medicine* 29, 373–386.

546 Kaufman MP & Forster HV (1996). *Reflexes Controlling Circulatory, Ventilatory and Airway
547 Responses to Exercise*. John Wiley & Sons, Inc., Hoboken, NJ, USA.

548 Kleckner IR, Zhang J, Touroutoglou A, Chanes L, Xia C, Simmons WK, Quigley KS, Dickerson
549 BC & Feldman Barrett L (2017). Evidence for a large-scale brain system supporting
550 allostasis and interoception in humans. *Nat hum behav* 1, 0069–15.

551 Lang PJ, Wangelin BC, Bradley MM, Versace F, Davenport PW & Costa VD (2011). Threat of
552 suffocation and defensive reflex activation. *Psychophysiol* 48, 393–396.

553 Lansing RW, Im B, Thwing JI, Legedza A & Banzett RB (2000). The perception of respiratory
554 work and effort can be independent of the perception of air hunger. *Am J Respir Crit Care*

555 Med 162, 1690–1696.

556 Ling S & Carrasco M (2006). When sustained attention impairs perception. *Nat Neurosci* 9,
557 1243–1245.

558 Mallorqui-Bague N, Bulbena A, Pailhez G, Garfinkel SN & Critchley HD (2016). Mind-Body
559 Interactions in Anxiety and Somatic Symptoms. *Harvard Review of Psychiatry* 24, 53–60.

560 McKay LC, Adams L, Frackowiak RSJ & Corfield DR (2008). A bilateral cortico-bulbar
561 network associated with breath holding in humans, determined by functional magnetic
562 resonance imaging. *NeuroImage* 40, 1824–1832.

563 Merikle PM & Joordens S (1997). Parallels between Perception without Attention and
564 Perception without Awareness. *Consciousness and cognition* 6, 219–236.

565 Miller KL et al. (2016). Multimodal population brain imaging in the UK Biobank prospective
566 epidemiological study. *Nat Neurosci* 19, 1523–1536.

567 Parshall MB, Schwartzstein RM, Adams L, Banzett RB, Manning HL, Bourbeau J, Calverley
568 PM, Gift AG, Harver A, Lareau SC, Mahler DA, Meek PM & O'Donnell DE (2012). An
569 Official American Thoracic Society Statement: Update on the Mechanisms, Assessment, and
570 Management of Dyspnea. *Am J Respir Crit Care Med* 185, 435–452.

571 Pattinson K, Mitsis GD, Harvey AK & Jbabdi S (2009a). Determination of the human brainstem
572 respiratory control network and its cortical connections in vivo using functional and
573 structural imaging. *NeuroImage* 44, 295–305.

574 Pattinson KTS, Governo RJ, MacIntosh BJ, Russell EC, Corfield DR, Tracey I & Wise RG
575 (2009b). Opioids Depress Cortical Centers Responsible for the Volitional Control of
576 Respiration. *Journal of Neuroscience* 29, 8177–8186.

577 Paulus MP, Flagan T, Simmons AN, Gillis K, Kotturi S, Thom N, Johnson DC, Van Orden KF,
578 Davenport PW & Swain JL (2012). Subjecting Elite Athletes to Inspiratory Breathing Load
579 Reveals Behavioral and Neural Signatures of Optimal Performers in Extreme Environments
580 ed. Lucia A. *PLoS ONE* 7, e29394.

581 Pavlov IP (1927). Conditioned Reflexes.

582 Phelps EA, Ling S & Carrasco M (2006). Emotion facilitates perception and potentiates the
583 perceptual benefits of attention. *Psychol Sci* 17, 292–299.

584 Porro CA, Baraldi P, Pagnoni G, Serafini M, Facchin P, Maierón M & Nichelli P (2002). Does
585 anticipation of pain affect cortical nociceptive systems? *The Journal of Neuroscience* 22,
586 3206–3214.

587 Price DD, Milling LS, Kirsch I, Duff A, Montgomery GH & Nicholls SS (1999). An analysis of
588 factors that contribute to the magnitude of placebo analgesia in an experimental paradigm.
589 *Pain* 83, 147–156.

590 Simmons WK, Avery JA, Barcalow JC, Bodurka J, Drevets WC & Bellgowan P (2012). Keeping
591 the body in mind: Insula functional organization and functional connectivity integrate
592 interoceptive, exteroceptive, and emotional awareness. *Human brain mapping* 34, 2944–
593 2958.

594 Smith SM (2002). Fast robust automated brain extraction. *Human brain mapping* 17, 143–155.

595 Smith SM, Fox PT, Miller KL, Glahn DC, Fox PM, Mackay CE, Filippini N, Watkins KE, Toro
596 R, Laird AR & Beckmann CF (2009). Correspondence of the brain's functional architecture
597 during activation and rest. 1–6.

598 Smith SM, Nichols TE, Vidaurre D, Winkler AM, Behrens TEJ, Glasser MF, Ugurbil K, Barch
599 DM, Van Essen DC & Miller KL (2015). A positive-negative mode of population
600 covariation links brain connectivity, demographics and behavior. *Nature Med* 18, 1565–1567.

601 Spinhoven P, vanPeskiOosterbaan AS, VanderDoes A, Willems L & Sterk PJ (1997).
602 Association of anxiety with perception of histamine induced bronchoconstriction in patients
603 with asthma. *Thorax* 52, 149–152.

604 Takano N, Inaishi S & Zhang Y (1997). Individual differences in breathlessness during exercise,
605 as related to ventilatory chemosensitivities in humans. *The Journal of Physiology* 499, 843–
606 848.

607 Tang J & Gibson S (2005). A Psychophysical Evaluation of the Relationship Between Trait
608 Anxiety, Pain Perception, and Induced State Anxiety. *The Journal of Pain* 6, 612–619.

609 Van den Bergh O, Withöft M, Petersen S & Brown RJ (2017). Symptoms and the body: Taking
610 the inferential leap. *Neuroscience & Biobehavioral Reviews* 74, 185–203.

611 Van Den Heuvel MP & Pol HEH (2010). Exploring the brain network: a review on resting-state
612 fMRI functional connectivity. *European Neuropsychopharmacology* 20, 519–534.

613 Vossel S, Geng JJ & Fink GR (2014). Dorsal and Ventral Attention Systems: Distinct Neural
614 Circuits but Collaborative Roles. *Neuroscientist* 20, 150–159.

615 Wager TD, Rilling JK, Smith EE, Sokolik A, Casey KL, Davidson RJ, Kosslyn SM, Rose RM &
616 Cohen JD (2004). Placebo-Induced Changes in fMRI in the Anticipation and Experience of
617 Pain. *Science* 303, 1162–1167.

618 Wager TD, Waugh CE, Lindquist M, Noll DC, Fredrickson BL & Taylor SF (2009). Brain
619 mediators of cardiovascular responses to social threat. *NeuroImage* 47, 821–835.

620 Waldrop TG, Eldridge FL, Iwamoto GA & Mitchell JH (2010). Central Neural Control of
621 Respiration and Circulation During Exercise, 2nd edn. John Wiley & Sons, Inc., Hoboken,
622 NJ, USA.

623 Winkler AM, Ridgway GR, Webster MA, Smith SM & Nichols TE (2014). Permutation
624 inference for the general linear model. *NeuroImage* 92, 381–397.

625 Woolrich MW, Behrens TEJ, Beckmann CF, Jenkinson M & Smith SM (2004). Multilevel linear
626 modelling for fMRI group analysis using Bayesian inference. *NeuroImage* 21, 1732–1747.

627 Woolrich MW, Ripley BD, Brady M & Smith SM (2001). Temporal Autocorrelation in
628 Univariate Linear Modeling of fMRI Data. *NeuroImage* 14, 1370–1386.

629

Tables

630
631
632

633 **Table 1.** Mean (\pm sd) physiological variables across conditioned respiratory tasks. *Significantly
634 ($p < 0.05$) different from sedentary group. Abbreviations: $P_{ET}CO_2$, pressure of end-tidal carbon
635 dioxide; $P_{ET}O_2$, pressure of end-tidal oxygen; RVT, respiratory volume per unit time; bpm, beats
636 per minute.

	Unloaded breathing		Anticipation		Breathlessness	
	ATHLETE	SEDENTARY	ATHLETE	SEDENTARY	ATHLETE	SEDENTARY
$P_{ET}CO_2$ (mmHg)	35.96 (5.56)	35.08 (3.20)	35.50 (5.81)	34.76 (3.60)	36.34 (6.23)	35.40 (3.92)
$P_{ET}O_2$ (mmHg)	129.68 (6.41)	134.09 (15.15)	129.55 (6.75)	133.59 (13.47)	131.18 (6.83)	137.55 (16.42)
Respiratory rate (min^{-1})	10.15 (2.59)*	13.35 (3.51)	9.99 (2.63)*	12.93 (4.29)	9.40 (3.58)	11.54 (5.11)
RVT (% change from baseline)	-4.06 (5.70)	-0.56 (7.94)	-0.03 (12.14)	6.07 (18.78)	-20.00 (24.88)	-13.23 (28.54)

637

638

639

640 **Table 2.** Mean (\pm sd) physiological and psychological variables during breathlessness for both
641 athletes and sedentary subjects.

	ATHLETE	SEDENTARY
Peak mouth pressure (cmH_2O)	14.4 (8.5)	12.0 (5.8)
Breathlessness intensity rating (%)	46.3 (14.1)	46.7 (18.1)
Breathlessness anxiety rating (%)	31.9 (17.8)	36.1 (20.0)
Unloaded breathing intensity rating (%)	2.3 (3.5)	3.4 (3.4)
Unloaded breathing anxiety rating (%)	2.8 (4.8)	2.2 (2.7)

642

643
644
645

Figure legends

646 **Figure 1. Mean BOLD activity in athletes and sedentary controls.** Top: BOLD activity
647 during conditioned anticipation of breathlessness. Bottom: BOLD activity during a
648 breathlessness challenge, induced via inspiratory resistive loading. The images consist of a
649 colour-rendered statistical map superimposed on a standard (MNI 1x1x1 mm) brain, and
650 significant regions are displayed with a non-parametric cluster probability threshold of $t < 3.1$; p
651 < 0.05 (corrected for multiple comparisons). Abbreviations: M1, primary motor cortex; SMC,
652 supplementary motor cortex; dACC, dorsal anterior cingulate cortex; PCC, posterior cingulate
653 cortex; dlPFC, dorsolateral prefrontal cortex; a-In, anterior insula; OP, operculum; amyg,
654 amygdala; hipp, hippocampus; Crus-I, cerebellar lobe; activation, increase in BOLD signal;
655 deactivation, decrease in BOLD signal.

656
657

658 **Figure 2. Interaction between groups and breathlessness scores.** Left: BOLD activity during
659 conditioned anticipation of breathlessness. Red-yellow = BOLD activity correlating with
660 intensity scores in athletes > sedentary subjects; blue-light blue = BOLD activity correlating with
661 anxiety scores in sedentary > athletic subjects. Right: Percentage BOLD signal change within the
662 (red-yellow) intensity-correlated imaging mask against intensity scores, demonstrating a positive,
663 linear correlation in athletes and a negative relationship in sedentary subjects. The images consist
664 of a colour-rendered statistical map superimposed on a standard (MNI 1x1x1 mm) brain, and
665 significant regions are displayed with a non-parametric cluster probability threshold of $t < 3.1$; p
666 < 0.05 (corrected for multiple comparisons). Abbreviations: M1, primary motor cortex; a-In,
667 anterior insula; m-In, middle insula; hipp, hippocampus; put, putamen; CN, caudate nucleus;
668 VPL, ventral posterolateral thalamic nucleus.

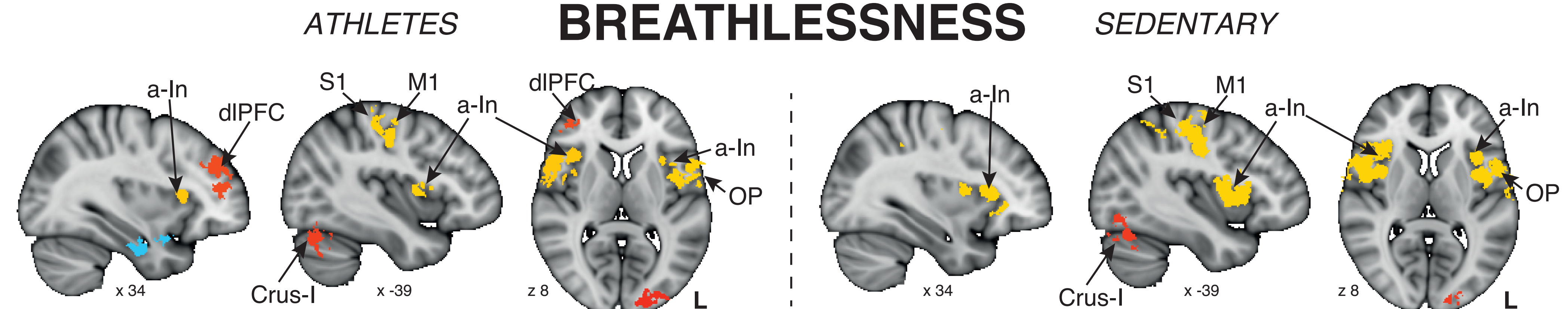
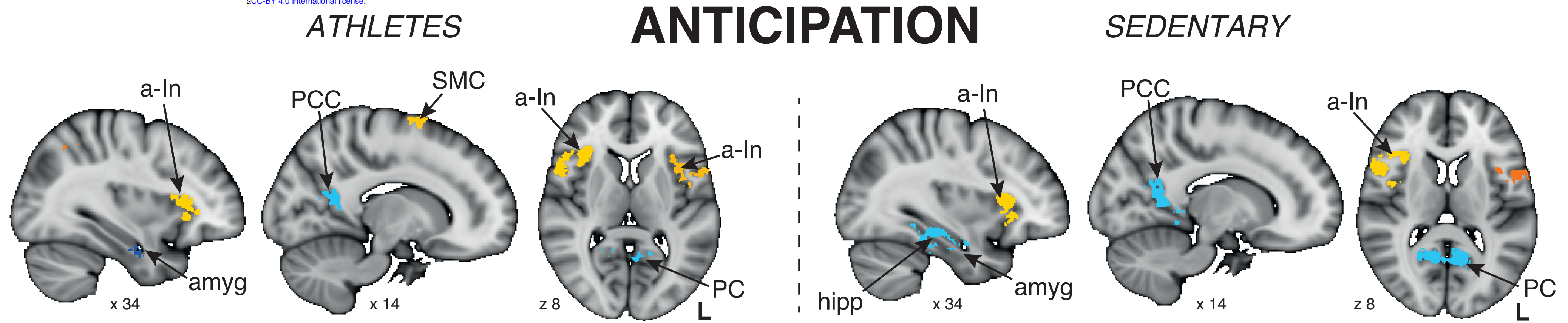
669
670

671 **Figure 3. Differences in resting functional connectivity between athletes and sedentary**
672 **subjects.** Increased functional connectivity (purple) observed in athletes between an area of
673 primary motor cortex that is active during breathlessness (right) and a cingulo-opercular task-
674 positive network (left) identified at rest. The images consist of a colour-rendered statistical map
675 superimposed on a standard (MNI 1x1x1 mm) brain, and significant regions are displayed with a
676 non-parametric cluster probability threshold of $t < 3.1$; $p < 0.05$ (corrected for multiple
677 comparisons).

678
679

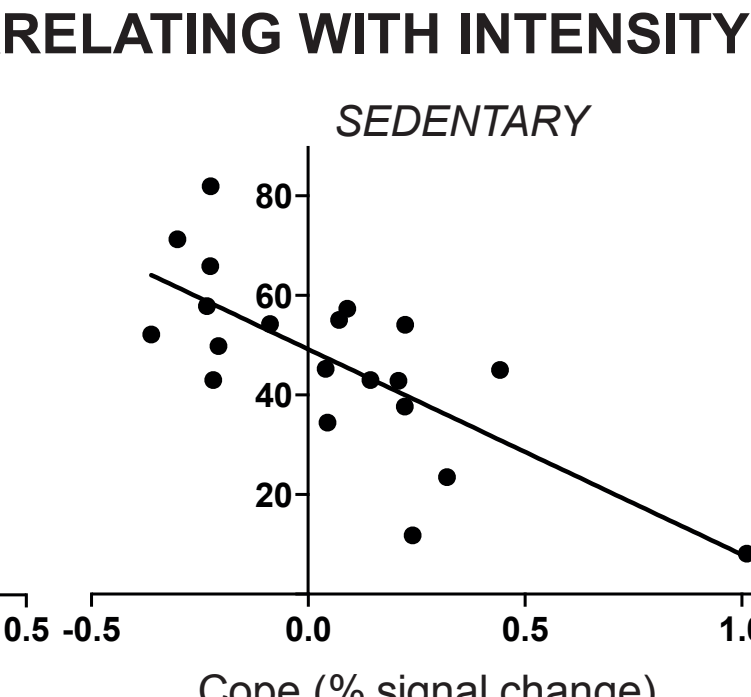
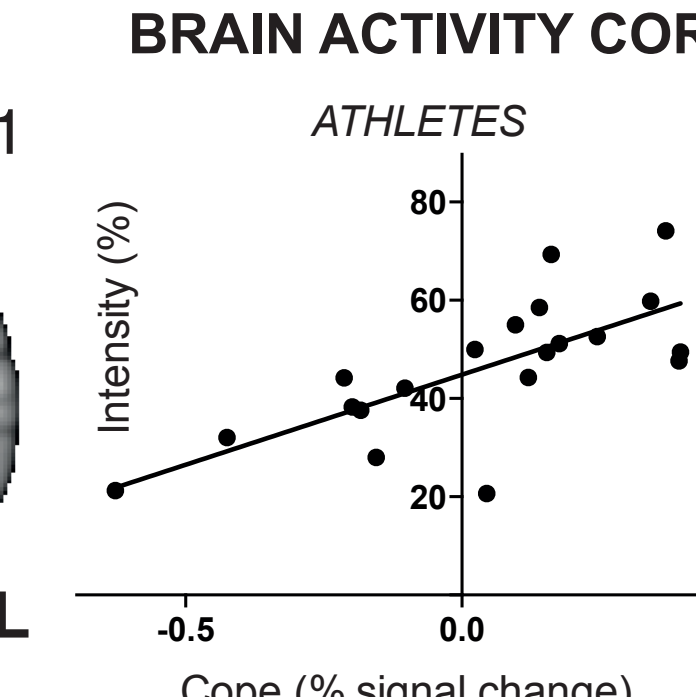
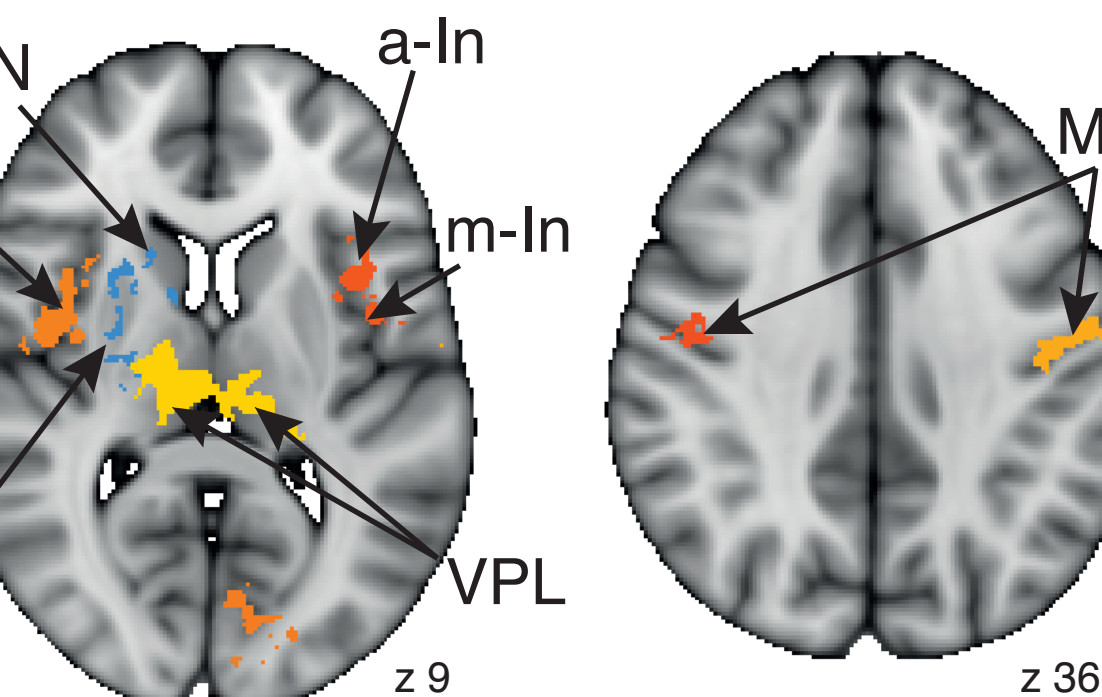
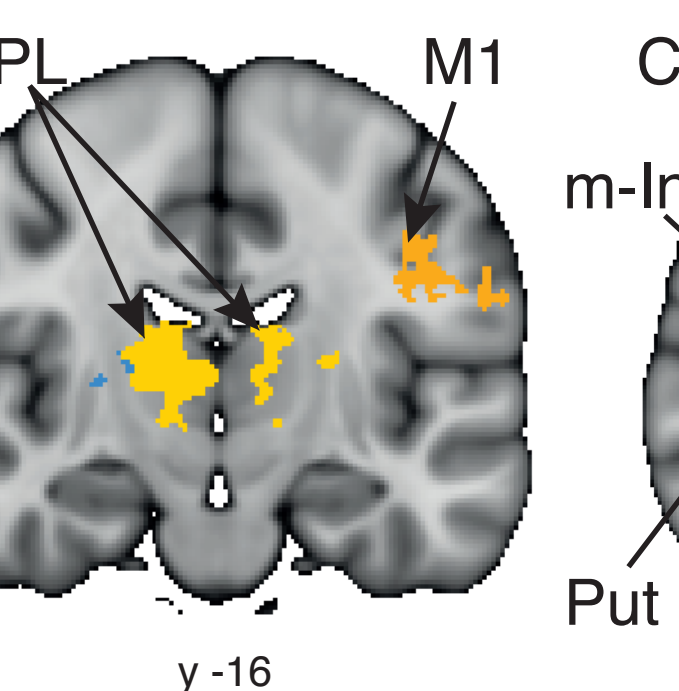
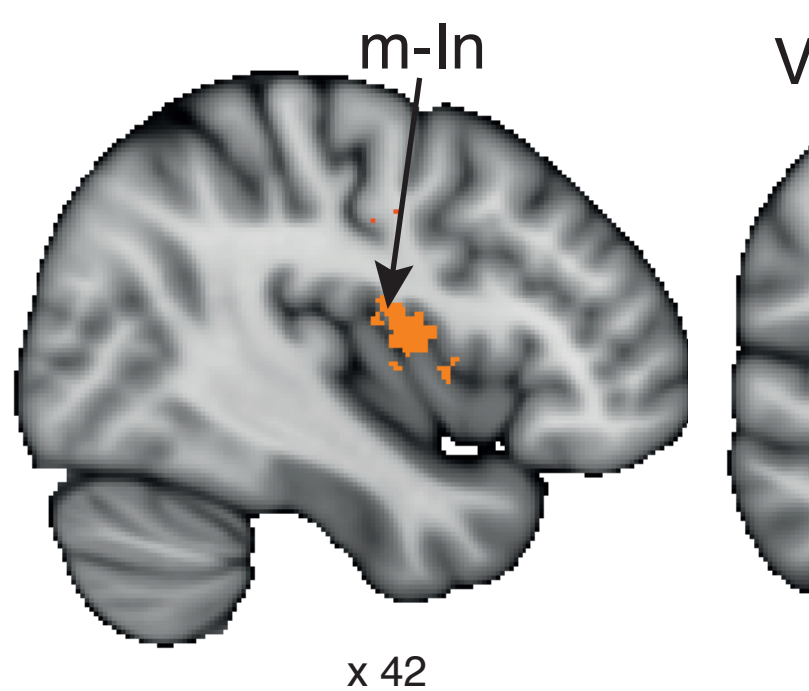
680 **Figure 4. Previously reported differences in ventilatory perceptions between athletes and**
681 **sedentary subjects. *Significantly different slope from sedentary subjects.** Subject-specific
682 change in breathlessness anxiety and intensity scores plotted against percentage change in
683 ventilation from baseline, induced by both mild (top) and moderate (bottom) hypercapnia (mild
684 hypercapnia: aim of 0.8%; and moderate hypercapnia: aim of 1.5% increase in end-tidal carbon

685 dioxide, end-tidal oxygen was maintained constant). Athletes are plotted in the left column, and
686 sedentary subjects in the right column. During both mild and moderate hypercapnia, the athlete
687 group showed a positive linear correlation between change in ventilation and change in breathing
688 anxiety that was significantly different from sedentary subjects (slope difference: mild $p = 0.018$;
689 moderate $p = 0.011$). Athletes also demonstrated significant positive correlations for
690 breathlessness intensity against change in ventilation, where the slope was significantly different
691 to sedentary subjects in moderate ($p = 0.047$) but not mild ($p = 0.177$) hypercapnia. 95%
692 Confidence intervals are shown. Figure is recreated from previously published data (Faull *et al.*,
693 2016a) under the Creative Commons license.

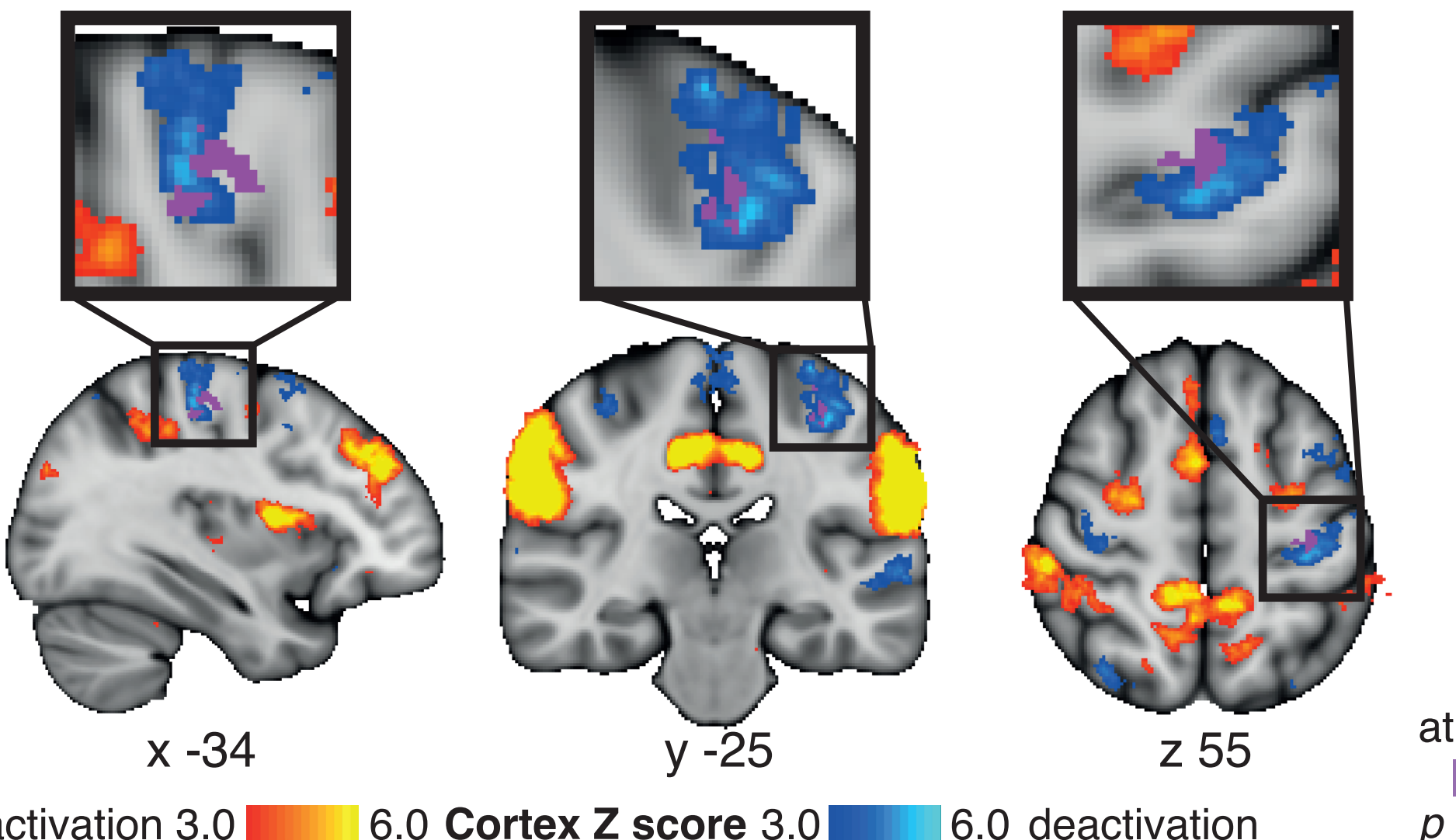


activation 0.05 <0.001 Cortex p value 0.05 <0.001 deactivation

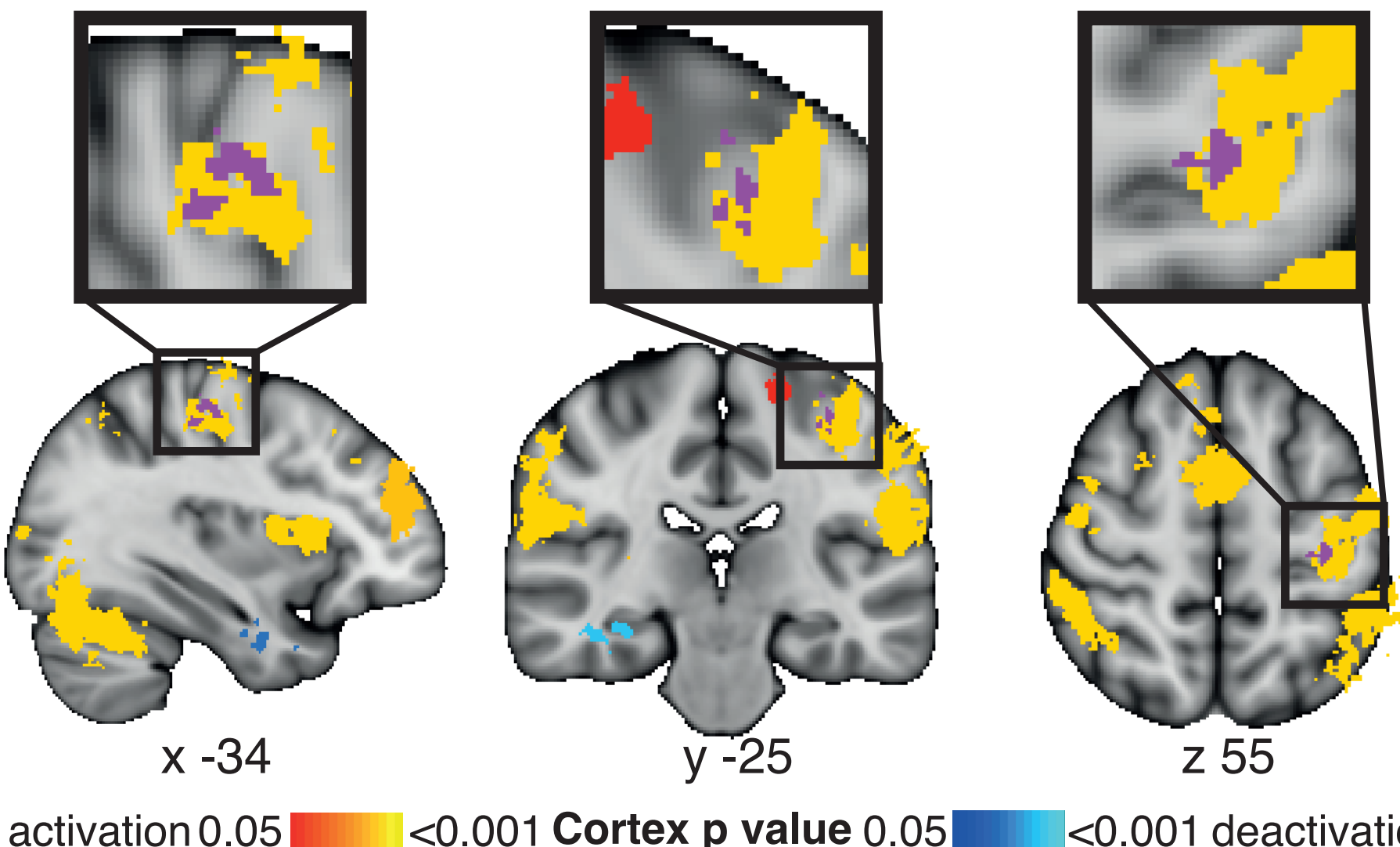
ANTICIPATION SCALING WITH BREATHLESSNESS SCORES



TASK-POSITIVE NETWORK

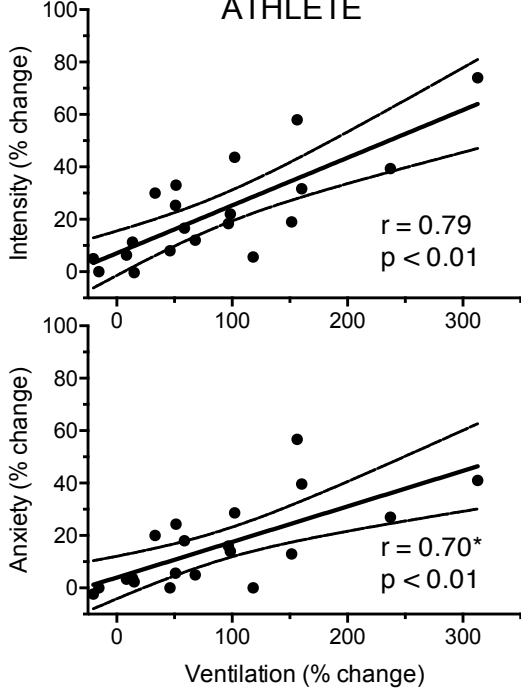


BREATHLESSNESS

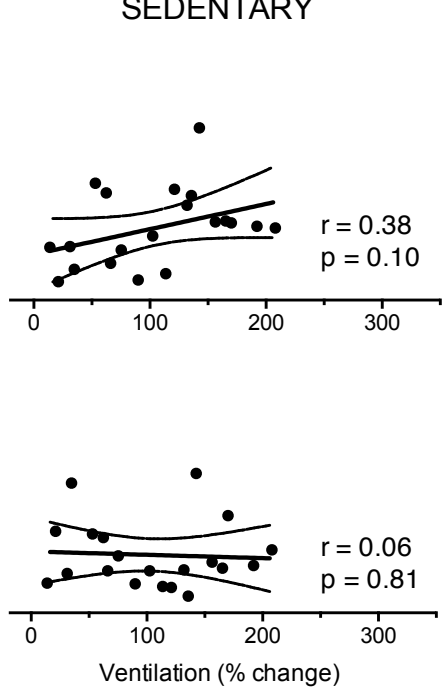


MILD HYPERCAPNIA

ATHLETE

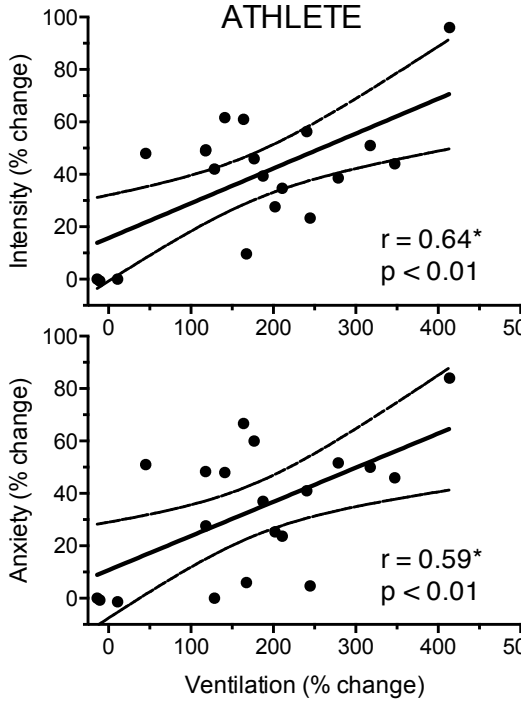


SEDENTARY



MODERATE HYPERCAPNIA

ATHLETE



SEDENTARY

